

Published in final edited form as:

Nanomedicine. 2015 January ; 11(1): 31–38. doi:10.1016/j.nano.2014.07.004.

Polysilsesquioxane Nanoparticles for Triggered Release of Cisplatin and Effective Cancer Chemoradiotherapy

Joseph Della Rocca, Ph.D.^a, Michael E. Werner, Ph.D.^b, Stephanie A. Kramer, B.S.^a, Rachel C. Huxford-Phillips, B.S.^a, Rohit Sukumar, B.S.^b, Natalie D. Cummings, B.A.^b, Juan L. Vivero-Escoto, Ph.D.^a, Andrew Z. Wang, M.D.^{b,c,*}, and Wenbin Lin, Ph.D.^{a,c,d,*}

^aDepartment of Chemistry, University of North Carolina, Chapel Hill, NC 27599

^bLaboratory of Nano- and Translational Medicine, Department of Radiation Oncology, CB 7512 University of North Carolina School of Medicine, Chapel Hill, NC 27599, USA

^cLineberger Comprehensive Cancer Center, University of North Carolina School of Medicine, Chapel Hill, NC 27599, USA

^dDepartment of Chemistry, University of Chicago, 929 East 56th St, Chicago, IL 60637, USA

Abstract

Chemoradiotherapy is a well-established treatment paradigm in oncology. There has been strong interest in identifying strategies to further improve its therapeutic index. An innovative strategy is to utilize nanoparticle (NP) chemotherapeutics in chemoradiation. Since the most commonly utilized chemotherapeutic with radiotherapy is cisplatin, the development of a NP cisplatin for chemoradiotherapy has the highest potential impact on this treatment. Here, we report the development of a NP comprised of polysilsesquioxane (PSQ) polymer crosslinked by a cisplatin prodrug (Cisplatin-PSQ) and its utilization in chemoradiotherapy using non-small cell lung cancer as a disease model. Cisplatin-PSQ NP has an exceptionally high loading of cisplatin. Cisplatin-PSQ NPs were evaluated in chemoradiotherapy *in vitro* and *in vivo*. They demonstrated significantly higher therapeutic efficacy when compared to cisplatin. These results suggest that the Cisplatin-PSQ NP holds potential for clinical translation in chemoradiotherapy.

Keywords

hybrid nanomaterials; nanomedicine; cancer chemoradiotherapy; cisplatin; polysilsesquioxane; lung cancer; silica

© 2014 Elsevier Inc. All rights reserved.

Corresponding Authors: Andrew Zhuang Wang, Department of Radiation Oncology, Lineberger Comprehensive Cancer Center, CB 7512, UNC Chapel Hill, Chapel Hill, North Carolina, 27514, (P) 919-966-7700, (F) 919-966-7681, zawang@med.unc.edu. Wenbin Lin, Department of Chemistry, University of Chicago, 929 East 56th St, Chicago, IL 60637, USA, (P) (773) 834-7163, wenbinlin@uchicago.edu.

Disclosure of potential conflicts of interest

W.L. and A.Z.W. are co-founders of Coordination Therapeutics, Inc.

Publisher's Disclaimer: This is a PDF file of an unedited manuscript that has been accepted for publication. As a service to our customers we are providing this early version of the manuscript. The manuscript will undergo copyediting, typesetting, and review of the resulting proof before it is published in its final citable form. Please note that during the production process errors may be discovered which could affect the content, and all legal disclaimers that apply to the journal pertain.

1. Background

Chemoradiotherapy, the concurrent administration of chemotherapy and radiotherapy, is part of the standard of care curative treatment for many difficult to treat solid cancers, including brain, head and neck, esophageal, gastric, pancreatic, lung, rectal, anal, and cervical cancers.^{1–5} Chemoradiotherapy has been shown to consistently improve local tumor control and rates of cancer cure compared to either sequential treatment or sole administration of chemotherapy or radiotherapy. Given its importance, one of the key aims in oncology research has been to identify agents and methods to improve chemoradiotherapy.⁶ Current approaches have focused on utilizing biologics to improve chemoradiotherapy. Unfortunately, the improvements have been modest.⁷ Advances in drug delivery and nanomedicine have offered an unprecedented opportunity to improve chemoradiotherapy.⁸ Nanoparticle (NP) possesses a unique biodistribution profile that is ideally suited for delivering chemotherapy agents for chemoradiotherapy. NPs preferentially accumulate in tumors through the enhanced permeability and retention (EPR) effect.^{9, 10} This leads to a higher intratumoral drug concentration when compared to their small molecule chemotherapeutic counterparts. Furthermore, NPs are unable to penetrate normal vasculatures and capillaries, leading to a lower dose to normal, healthy tissues near the tumor. This allows for a greater drug concentration differential between the tumor and surrounding normal tissue, which can translate into a higher therapeutic index. Indeed, preclinical studies have suggested that NP therapeutics are more effective than small molecule chemotherapeutics in chemoradiotherapy.^{8, 11–13}

The most commonly utilized chemotherapeutic in chemoradiation is cisplatin.^{14, 15} While highly effective, its use and efficacy has been limited by toxicity.¹⁴ Therefore, improving cisplatin-based chemoradiotherapy will have the greatest clinical impact on chemoradiotherapy. We have recently developed a new NP platform, known as polysilsesquioxane (PSQ) NP, for the delivery of an oxaliplatin prodrug¹⁶. We hypothesized that we can formulate a PSQ NP of cisplatin as an improved chemotherapeutic agent compared to cisplatin. This would also allow the PSQ NP platform to have a broader clinical indication. Herein, we report the synthesis and characterization of Cisplatin-PSQ NP with extremely high cisplatin loadings and trigger release properties. The NP was also post-synthetically modified with a polyethylene glycol (PEG) shell to allow for superior *in vivo* performance. The potential of Cisplatin-PSQ NP in chemoradiotherapy was also demonstrated using non-small cell lung cancer (NSCLC) mouse models.

2. Materials and Methods

Materials

All chemicals were purchased from Fisher Scientific or Sigma-Aldrich and used without further purification unless noted. Cisplatin was purchased from AK Scientific. Tetrahydrofuran (THF) was distilled over sodium metal and benzophenone under nitrogen. Dimethylformamide (DMF) was dried by running through an activated alumina column. Thermogravimetric analysis (TGA) was performed using a Shimadzu TGA-50 equipped with a platinum pan and heated at 3 °C per minute in air. A JEM 100CX-2 transmission electron microscope (TEM) and a Hitachi S-4700 scanning electron microscope (SEM) were

used to determine particle size and morphology. TEM and SEM samples were prepared from ethanolic suspensions of the NPs dropped onto amorphous carbon coated copper grids or glass slides. The solvent was then allowed to evaporate. Dynamic light scattering (DLS) and zeta potential were measured using a Malvern Instrument Zetasizer Nano. Inductively-coupled plasma mass spectrometry (ICP-MS) measurements were obtained using a Varian 820-MS Inductively-Coupled Plasma Mass Spectrometer. ICP-MS samples were prepared by digesting a known amount of sample in concentrated nitric acid overnight, and then diluting with water to 2% nitric acid by volume.

NCI-H460 human NSCLC (ATCC# HTB-177), A549 human lung carcinoma cells (ATCC# CCL-185), and all cell culture reagents were purchased from the Tissue Culture Facility of the Lineberger Comprehensive Cancer Center at UNC-Chapel Hill. All cells were maintained at 37 °C with 5% CO₂ and were cultured according to ATCC recommendations. Mice (male nu/nu, 4–6 weeks old) were purchased from the animal colony at the UNC Lineberger Comprehensive Cancer Center. Mice were housed in an AALAC accredited facility in sterile housing at UNC-Chapel Hill. All animal work was approved and monitored by the UNC-Chapel Hill Institutional Animal Care and Use Committee.

Synthesis

Synthesis of *c,c,t*-Pt(NH₃)₂Cl₂(propyltriethoxysilane succinic acid)₂ (DSCP-Si)

—The platinum precursor complex *c,c,t*-Pt(NH₃)₂Cl₂(OH)₂ was synthesized from cisplatin according to a previously published method¹⁷. Two hundred milligrams of *c,c,t*-Pt(NH₃)₂Cl₂(OH)₂ (0.6 mmol) was suspended in 4 mL of anhydrous DMF. 700 μL of 3-(triethoxysilyl)propyl succinic anhydride was then added (1.8 mmol). The resulting suspension was stirred under argon at 50 °C for 3 days, yielding a clear yellow solution. Two volume equivalents of triethylamine were added to precipitate the product. The product was isolated by centrifugation and washed twice with diethyl ether before drying under high vacuum, yielding a yellow brown crystalline material. The product was stored at –20 °C. Yield: 440 mg (78%). ¹H NMR (DMSO-*d*⁶): 6.25(6H, NH₃), 3.73 (12H, OCH₂), 2.75 (4H, CH₂), 2.31 (2H, CH), 1.45 (4H, CH₂), 1.32 (4H, CH₂), 1.12 (18H, CH₃), 0.52 (4H, CH₂).

Synthesis of Amino-Polyethylene-glycol (MW=5000) monomethyl ether

(PEG₅₀₀₀-NH₂)—Polyethylene glycol (PEG) (MW=5000) monomethyl ether (30 g) was dried under vacuum at 90 °C overnight. Anhydrous THF (360 mL) was added, followed by 3.6 mL (46.5 mmol) of methanesulfonyl chloride. The solution was cooled to 0 °C on an ice bath and 6.9 mL triethylamine dissolved in 60 mL THF was added dropwise. The ice bath was removed, and the resulting solution was stirred under nitrogen at room temperature overnight. Water (150 mL) was added and the solution was cooled back to 0 °C. A sodium bicarbonate solution (1 M, 15 mL) and sodium azide (3.9 g, 60 mmol) were added. The THF was removed by rotary evaporation and the remaining aqueous solution was refluxed for 24 hours. PEG-azide was extracted with dichloromethane (4×100 mL). The organic layers were collected, concentrated, and extracted with brine. The organic solution was then dried with magnesium sulfate, filtered, and then the dichloromethane was removed by rotary evaporation (21.2 g, 70% yield). ¹H NMR (CDCl₃) δ 2.93(2H), 3.33 (3H), 3.42 (3H), 3.50 (4H), 3.53–3.75(410H), 3.77 (4H). The monomethyl PEG-azide complex (6.083 g) was

heated to 80 °C before being dissolved into 115 mL of THF and triphenylphosphine (3.174 g, 12.1 mmol) was added. The solution was stirred at room temperature for 12 hours. Water (9.1 mL) was then added and the solution was stirred for 18 hours. The THF was removed by rotary evaporation and the residue was dissolved in water (150 mL), precipitating triphenylphosphine oxide. The triphenylphosphine byproducts were removed by filtration, and the water was removed by rotary evaporation. (3.95 g, 65% yield). ¹H NMR (CDCl₃): 2.95 (2H), 3.32 (3H), 3.41(4H), 3.49 (4H), 3.50–3.70 (436H), 3.76 (4H).

Synthesis of Cisplatin-PSQ—DSCP-Si was dissolved in a mixture of ethanol, ammonium hydroxide solution (33%), and water (2:1:1.5). The resulting solution was stirred at room temperature in the dark for 1 hour. The resulting bluish white NP suspension was loaded onto a cation exchange column (Amberlite IRC-50) and the NPs were eluted using water. Residual impurities were removed by dialysis against water. Cisplatin-PSQ was isolated by centrifugation, washed with ethanol, and stored as an ethanolic suspension.

PEG Conjugation—Cisplatin-PSQ was suspended into acetonitrile at 1 mg/mL. To the Cisplatin-PSQ suspension, PEG₅₀₀₀-NH₂ (1 mM), triethylamine (18 mM) and HBTU (8 mM) were added. The suspension was stirred at room temperature for 24 hours before the NPs were isolated by centrifugation, and washed with acetonitrile twice and ethanol once. PEG-Cisplatin-PSQ was stored as an ethanolic suspension.

Platinum Release from Cisplatin-PSQ

400 mL of 2 mM HEPES buffer (pH=7.4) was placed in a 2-neck round bottom flask and then sparged with nitrogen gas and pre-warmed to 37 °C. Cisplatin-PSQ (2 mg, 1.84 μmol Pt) was suspended into 2 mL of the buffer solution. The NP suspension was then added to the large buffer sink and the system was incubated at 37 °C under a N₂ blanket. Periodically, 1.2 mL aliquots of the solution were removed. After 1 day of incubation, a solution of *L*-cysteine in 2 mM HEPES buffer was added to make the total reducing agent concentration either 5 mM or 15 μM. The resulting system was incubated at 37 °C, with 1.2 mL aliquots periodically removed. The removed aliquots were processed by filtering the suspensions through a Costar Spin-X centrifuge tube filter (0.22 μm cellulose acetate). The filtrate was collected and analyzed by ICP-MS.

Cell Viability Assay Studies

A549 cells—A549 cells were plated in 6 well plates at 100,000 cells/well and incubated in 3 mL media for 12 hours to promote cell attachment. The plates were washed once with 2 mL PBS and subsequently given 2 mL media containing varying drug concentrations. The plates were incubated at 37 °C for 48 hours before the media was replaced with 2 mL of fresh media. The plates were incubated for an additional 24 hours before cell viability was determined by the trypan blue dye exclusion assay.

NCI-H460 cells—NCI-H460 cells were plated in 6 well plates at 300,000 cells/well and incubated in 3 mL media for 12 hours to promote cell attachment. The plates were then washed once with 2 mL PBS and subsequently given 2 mL of media containing varying

drug concentrations. The plates were incubated at 37 °C for 48 hours and cell viability was determined by the trypan blue dye exclusion assay.

Clonogenic Survival Assay-Chemoradiation Therapy

A549 cells in 10 cm² plastic dishes were treated with 0.5 μM PEG-Cisplatin-PSQ or Cisplatin for 48 hours. After treatment, cells were washed with PBS, trypsinized, and seeded in 25 mL flasks at various densities. The flasks were then radiated immediately at 0, 2, 4, 6, or 8 Gy. Cells were incubated in the flasks for 10 days after irradiation. After incubation, cells were fixed in a 1:1 acetone:methanol mixture, and stained with trypan blue. All colonies with over 50 cells were counted. The relative cell surviving fraction was calculated by dividing the number of colonies of radiated cells by the number of cells plated, with a correction for the plating efficiency.

Tumor Efficacy Studies-Chemoradiation Therapy

Animal experiments were conducted in accordance to a protocol that was approved by the UNC Institutional Animal Use and Care review committee. A549 or NCI-H460 cells (1×10⁶ cells in 200 μL 1:1 RPMI-1640 and matrigel) were subcutaneously injected in the upper dorsal region of 6–8 week old Nu/Nu mice. Twelve days after inoculation, the mice were randomly distributed into different groups for subsequent treatment (PEG-Cisplatin-PSQ, free cisplatin, XRT only, and control) (7 mice per group). PEG-Cisplatin-PSQ or free cisplatin in PBS was tail vein i.v. injected at a dose of 1 mg cisplatin/kg. Six hours post injection, the tumors were subjected to a dose of 10 Gy with XRAD 320. Mice were shielded with a lead shield allowing radiation of the tumor site and minimal radiation to other organs. Tumor volumes were calculated by measuring two perpendicular diameters with a caliper and using the formula of $V=0.5 \times a \times b^2$, where 'a' and 'b' are the larger and smaller diameters, respectively. The tumor volumes were measured every 2 days, and the relative percent change in tumor volume was calculated using the relation $100 \times (V_i - V_o) / V_o$, where V_i is the volume calculated and V_o is the initial volume on day 1. Tumor volumes were compared at the end of the study using student t-test.

3. Results

Nanoparticle Synthesis

Cisplatin-PSQ NPs were synthesized via a base catalyzed sol-gel polymerization in a mixture of ethanol, water, and ammonia before purification by ion-exchange chromatography, dialysis, and centrifugation (Figure 1). These synthesis conditions are similar to those used in Stöber-type synthesis used to make monodisperse colloidal silica NPs.^{18, 19} The isolated NPs were characterized by transmission electron microscopy (TEM), scanning electron microscopy (SEM), dynamic light scattering (DLS), thermogravimetric analysis (TGA) and inductively coupled plasma-mass spectrometry (ICP-MS). Cisplatin-PSQ NPs have a diameter of 50–100 nm by both SEM and TEM (Figures 2A and 2B), but exhibit hydrogel-like behavior under physiological conditions, swelling to a DLS diameter (Z average) of 134.2 nm (Figure 2C, Table 1). TGA of Cisplatin-PSQ (Figure 2D) gives the expected weight loss for the completely condensed NP, indicating that Cisplatin-PSQ is a

homopolymer of DSCP-Si. ICP-MS measurements of the platinum content give a loading of 42 wt% cisplatin, confirming the TGA measurements.

Platinum Release from Cisplatin-PSQ

The platinum release from Cisplatin-PSQ was measured in the absence or presence of *L*-cysteine, a model reducing agent (Figure 3A). In the absence of any reducing agent ($t < 0$ hrs), only 9–15% of the total platinum is released, most likely from weakly physisorbed DSCP-Si on the NP surface which was quickly released after submersion in the buffer. After the addition of 15 μM *L*-cysteine, similar to the bloodstream thiol concentration, only a small amount of additional platinum is released over 73 hours of incubation. In contrast, platinum release is much more rapid in the presence of 5 mM *L*-cysteine, corresponding to the intracellular thiol concentration. All of the cisplatin payload was released in less than 48 h in the presence of 5 mM *L*-cysteine.

Post-synthetic modification of Cisplatin-PSQ

Amine-terminated polyethylene glycol (MW=5000) is coupled to the surface of Cisplatin-PSQ by an amide bond. The morphology of the NPs was unchanged by electron microscopy (Supporting Information), but the PEG-Cisplatin-PSQ NPs are 150 nm in diameter by DLS (Z average, Figure 2C, Table 1). The increase in hydrodynamic size is due to the polymer chains extending away from the NP surface. The zeta potential of PEG-Cisplatin-PSQ increased to -6.5 mV.

In vitro evaluation of PEG-Cisplatin-PSQ

PEG-Cisplatin-PSQ was evaluated *in vitro* against A549 and H460 lung cancer cells (Figure 3B and 3C). PEG-Cisplatin-PSQ has an IC_{50} of 14.9 μM against A549 cells and an IC_{50} of 2.07 μM against H460 cells, which are higher than those of cisplatin under the same conditions (IC_{50} of 3.5 μM against A549 cells and IC_{50} of 0.65 μM against H460 cells). PEG-Cisplatin-PSQ was also evaluated *in vitro* as a radiosensitizer (Figure 3D) against A549 cells. A549 cells were treated with 0.5 μM cisplatin or PEG-Cisplatin-PSQ, containing the equivalent of 0.5 μM cisplatin, 48 hours before being treated with varying doses of radiation. Cells treated with either platinum formulation plus radiation demonstrated less survival in a clonogenic assay than cells treated with radiation alone. This was consistent over all radiation dose levels tested.

In vivo evaluation of PEG-Cisplatin-PSQ in chemoradiotherapy

PEG-cisplatin-PSQ was studied *in vivo* in chemoradiotherapy in two mouse lung cancer xenograft models (Figures 4A and 4B). Mice received either no treatment, 10 Gy of radiotherapy, cisplatin (1 mg/kg) 6 hours prior to 10 Gy radiation, or PEG-Cisplatin-PSQ (1 mg cisplatin/kg) 6 hours prior to 10 Gy radiation. For the A549 xenograft model (Figure 4A), cisplatin treatment arm did not show any significant effects ($p > 0.05$) over radiation alone over the course of the study, while PEG-cisplatin-PSQ demonstrated a significant ($p < 0.05$) increase in efficacy over radiation alone from day 8 onwards as well as a significant improvement over cisplatin on day 22. The endpoint time (5x tumor volume increase for 1 mouse in group) was extended from 22 days for radiation only to 30 days for PEG-Cisplatin-

PSQ plus radiotherapy. For the H460 xenograft model (Figure 4B), cisplatin demonstrated insignificant radiosensitization effects over the course of the study. PEG-Cisplatin-PSQ demonstrated statistically significant ($p < 0.05$) increases in tumor growth inhibition over radiation alone over the entire study period and over cisplatin plus radiation from days 4–8 to days 14–16.

Discussions

The central aim of our study was to engineer a NP formulation of cisplatin that can improve the therapeutic efficacy of cisplatin-based chemoradiotherapy. We formulated the Cisplatin-PSQ NP and demonstrated that it has excellent physical properties (size and surface charge) for targeting tumors.²⁰ The size expansion of the PSQ NPs is due to the repulsive effects of the negatively charged silanols and carboxylic acids in the PSQ matrix, reflected in the highly negative zeta potential of Cisplatin-PSQ (Table 1). The Cisplatin-PSQ also has very high drug loading. This platinum loading corresponds to approximately 1.15×10^5 cisplatin molecules/NP and is several orders of magnitude higher than similar NP systems.^{21–25} The previously reported oxaliplatin-PSQ NPs have a comparable platinum loading on a number basis.¹⁶

One of the unique properties of Cisplatin-PSQ NP is its stability under normal physiological conditions. The NP is composed of large quantities of platinum (IV) centers, which are kinetically inert and must be reduced by biomolecules for the active platinum (II) complex to be released from the NP matrix in order to exert their antitumor activity (Figure 1). However, we expect Cisplatin-PSQ NPs to release cisplatin more rapidly within the tumor microenvironment or upon cellular internalization, where higher concentrations of reducing agents are present. Our drug release results have confirmed our hypothesis and that the Cisplatin-PSQ NPs would show minimal drug release in circulation, but when placed in a highly reducing environment, such as the tumor microenvironment or upon cellular internalization, cisplatin would be rapidly released from the PSQ matrix, leading to more pronounced antitumor effects.

For *in vivo* applications, we modified the Cisplatin-PSQ NP with polyethylene glycol (PEG). PEG is an inert, biocompatible polymer which is widely used to improve the biocompatibility, reduce mononuclear phagocytic system (MPS) uptake, and improve efficacy of nanomaterials.^{26–28} The presence of numerous carboxylic acids on the surface of Cisplatin-PSQ allows the NPs to be post-synthetically modified through standard amide coupling chemistry. The increase in surface charge of post-modified NPs is indicative of the neutral PEG chains shielding the NP surface charge and the replacement of anionic carboxylic acids with neutral amide linkages. Extrapolating TGA measurements (Figure 2D) gives a PEG coverage of 1 PEG/4.5 nm², which correlates to PEG in a brush confirmation extending away from the NP surface, which should impart sufficient stealth characteristics to the NPs.²⁹

In vitro evaluation of PEG-Cisplatin-PSQ as a chemotherapeutic and a radiosensitizer showed lower efficacy than that of cisplatin. This is presumably due to the presence of the PEG corona that can reduce the non-specific uptake of the NPs by the cancer cells, lowering

the intracellular cisplatin concentrations. The reducing power of standard cell media is quite low, so we would also expect minimal drug release in media. Our data is consistent with other NP formulations' result *in vitro*.³⁰

In contrast to *in vitro* results, PEG-Cisplatin-PSQ is significantly more effective than cisplatin in chemoradiotherapy. These results confirmed our hypothesis that NP formulations can improve chemoradiotherapy. It also suggest that PEG-Cisplatin-PSQ NPs hold high potential for clinical translation. The lack of therapeutic efficacy of small molecule cisplatin is likely due to the very low dose of drug we administered in this study. This also highlights the potency of PEG-Cisplatin-PSQ as a radiosensitizer. PEG-Cisplatin-PSQ presumably is able to accumulate in tumors more than cisplatin, which would allow the NP to exert a greater therapeutic effect. Studies are ongoing to further elucidate the pharmacokinetics, efficacy, and toxicity of PEG-Cisplatin-PSQ as a radiosensitizer and as a chemotherapy agent.

In summary, we have synthesized a novel NP formulation of cisplatin using base-catalyzed sol-gel polymerization. The Cisplatin-PSQ NPs have exceptionally high drug loading, and can be post-synthetically modified to possess a PEG surface. PEG-Cisplatin-PSQ was evaluated *in vitro* and *in vivo* in chemoradiotherapy using murine models of non-small cell lung cancer. PEG-Cisplatin-PSQ demonstrated higher therapeutic efficacy than cisplatin. These results suggest that Cisplatin-PSQ is a promising cancer therapeutic with the potential to significantly improve chemoradiotherapy for lung cancers as well as other solid tumor types.

Acknowledgments

Funding Source:

We acknowledge financial support from the N.I.H. (U54-CA151652 and U01-CA151455 to W.L. and R01CA178748-01 to AZW). A.Z.W was also supported by a NIH/NCI K12 Career Development Award (5-K12-CA120780-01-05), National Institutes of Health Center for Nanotechnology Excellence Grant 1-U54-CA151652-01, a Lung Cancer Foundation grant, and funds from the University Research Fund.

We thank technical support from the Animal Studies Core of the UNC Lineberger Cancer Center.

References

1. Brandsma D, Stalpers L, Taal W, Sminia P, van den Bent M. Clinical features, mechanisms, and management of pseudoprogression in malignant gliomas. *Lancet Oncology*. 2008; 9:453–61.
2. Chandana SR, Conley BA. Neoadjuvant chemotherapy for locally advanced squamous cancers of the head and neck: Current status and future prospects. *Current Opinion in Oncology*. 2009; 21:218–23. [PubMed: 19370805]
3. Ohe Y. Chemoradiotherapy for lung cancer. *Expert Opin Pharmacother*. 2005; 6:2793–804. [PubMed: 16318430]
4. Seiwert TY, Salama JK, Vokes EE. The concurrent chemoradiation paradigm—general principles. *Nat Clin Prac Oncol*. 2007; 4:86–100.
5. Willett CG, Czito BG. Chemoradiotherapy in gastrointestinal malignancies. *Clinical Oncology*. 2009; 21:543–56. [PubMed: 19577442]
6. Tepper JE, Wang AZ. Improving local control in rectal cancer: Radiation sensitizers or radiation dose? *J Clin Oncol*. 2010; 28:1623–4. [PubMed: 20194836]

7. Willett CG, Duda DG, di Tomaso E, Boucher Y, Czito BG, Vujaskovic Z, et al. Complete pathological response to bevacizumab and chemoradiation in advanced rectal cancer. *Nat Clin Pract Oncol.* 2007; 4:316–21. [PubMed: 17464339]
8. Werner ME, Foote MB, Wang AZ. Chemoradiotherapy of human tumors: Novel approaches from nanomedicine. *Curr Pharm Des.* 2012
9. Maeda H. Tumor-selective delivery of macromolecular drugs via the epr effect: Background and future prospects. *Bioconjugate Chemistry.* 2010; 21:797–802. [PubMed: 20397686]
10. Jain RK, Stylianopoulos T. Delivering nanomedicine to solid tumors. *Nat Rev Clin Oncol.* 2010; 7:653–64. [PubMed: 20838415]
11. Boulikas T. Clinical overview on lipoplatintm: A successful liposomal formulation of cisplatin. *Expert Opin Investig Drugs.* 2009; 18:1197–218.
12. Zhang X, Yang H, Gu K, Chen J, Rui M, Jiag G-L. In vitro and in vivo study of a nanoliposomal cisplatin as a radiosensitizer. *International Journal of Nanomedicine.* 2011; 6:437–44. [PubMed: 21499433]
13. Werner ME, Copp JA, Karve S, Cummings ND, Sukumar R, Li C, et al. Folate-targeted polymeric nanoparticle formulation of docetaxel is an effective molecularly targeted radiosensitizer with efficacy dependent on the timing of radiotherapy. *ACS Nano.* 2011; 5:8990–8. [PubMed: 22011071]
14. Kelland L. The resurgence of platinum-based cancer chemotherapy. *Nat Rev Cancer.* 2007; 7:573–84. [PubMed: 17625587]
15. Wheate NJ, Walker S, Craig GE, Oun R. The status of platinum anticancer drugs in the clinic and clinical trials. *Dalton Trans.* 2010; 39:8113–27. [PubMed: 20593091]
16. Della Rocca J, Huxford RC, Comstock-Duggan E, Lin W. Polysilsesquioxane nanoparticles for targeted platin-based chemotherapy by triggered release. *Angew Chem Int Ed.* 2011; 50:10330–4.
17. Rieter WJ, Pott KM, Taylor KML, Lin W. Nanoscale coordination polymers for platinum-based anticancer drug delivery. *J Am Chem Soc.* 2008; 130:11584–5. [PubMed: 18686947]
18. van Blaaderen, A.; Vrij, A. Synthesis and characterization of colloidal model particles made from organoalkoxysilanes. In: Bergna, HE.; Roberts, WO., editors. *Colloidal silica: Fundamentals and applications.* Boca Raton, FL: Taylor and Francis Group, LLC; 2006. p. 65-80.
19. Lu Y, McLellan J, Xia Y. Synthesis and crystallization of hybrid spherical colloids composed of polystyrene cores and silica shells. *Langmuir.* 2004; 20:3464–70. [PubMed: 15875883]
20. Sykes EA, Chen J, Zheng G, Chan WC. Investigating the impact of nanoparticle size on active and passive tumor targeting efficiency. *ACS Nano.* 2014
21. Peng X-H, Wang Y, Huang D, Wang Y, Shin HJ, Chen Z, et al. Targeted delivery of cisplatin to lung cancer using scfvegfr-heparin-cisplatin nanoparticles. *ACS Nano.* 2011; 5:9480–93. [PubMed: 22032622]
22. Avgoustakis K, Beletsi A, Panagi Z, Klepetsanis P, Karydas AG, Ithakissios DS. Plga-mpeg nanoparticles of cisplatin: In vitro nanoparticle degradation, in vitro drug release and in vivo drug residence in blood properties. *Journal of Controlled Release.* 2002; 79:123–35. [PubMed: 11853924]
23. Dhar S, Liu Z, Thomale J, Dai HJ, Lippard SJ. Targeted single-wall carbon nanotube-mediated pt(iv) prodrug delivery using folate as a homing device. *Journal of the American Chemical Society.* 2008; 130:11467–76. [PubMed: 18661990]
24. Feazell RP, Nakayama-Ratchford N, Dai H, Lippard SJ. Soluble single-walled carbon nanotubes as longboat delivery systems for platinum(iv) anticancer drug design. *Journal of the American Chemical Society.* 2007; 129:8438–9. [PubMed: 17569542]
25. Taylor-Pashow KML, Della Rocca J, Xie ZG, Tran S, Lin WB. Postsynthetic modifications of iron-carboxylate nanoscale metal-organic frameworks for imaging and drug delivery. *Journal of the American Chemical Society.* 2009; 131:14261–3. [PubMed: 19807179]
26. Alexis F, Pridgen E, Molnar LK, Farokhzad OC. Factors affecting the clearance and biodistribution of polymeric nanoparticles. *Molecular Pharmaceutics.* 2008; 5:505–15. [PubMed: 18672949]
27. Li S-D, Huang L. Pharmacokinetics and biodistribution of nanoparticles. *Molecular Pharmaceutics.* 2008; 5:496–504. [PubMed: 18611037]

28. Owens DE III, Peppas NA. Opsonization, biodistribution and pharmacokinetics of polymeric nanoparticles. *International Journal of Pharmaceutics*. 2006; 307:93–102. [PubMed: 16303268]
29. Jokerst JV, Lobovkina T, Zare RN, Gambhir SS. Nanoparticle pegylation for imaging and therapy. *Nanomedicine (London)*. 2011; 6:715–28.
30. Werner ME, Copp JA, Karve S, Cummings ND, Sukumar R, Li C, et al. Folate-targeted polymeric nanoparticle formulation of docetaxel is an effective molecularly targeted radiosensitizer with efficacy dependent on the timing of radiotherapy. *ACS Nano*. 2011; 5:8990–8. [PubMed: 22011071]

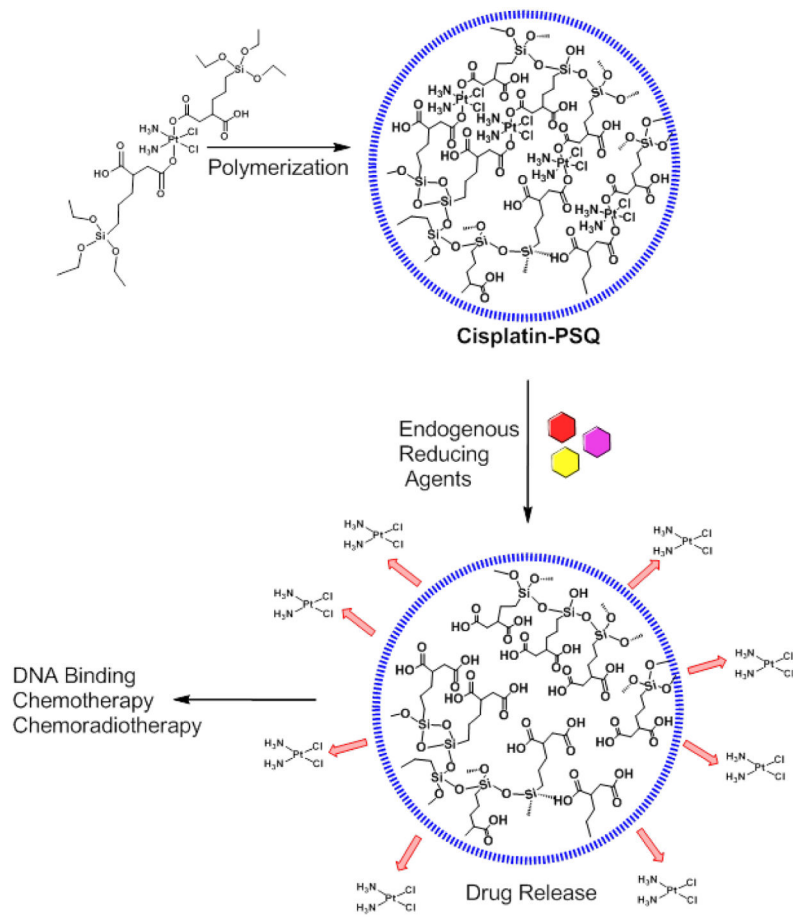


Figure 1. Schematic of the synthesis and triggered drug release of Cisplatin-PSQ nanoparticles for tumor growth inhibition.

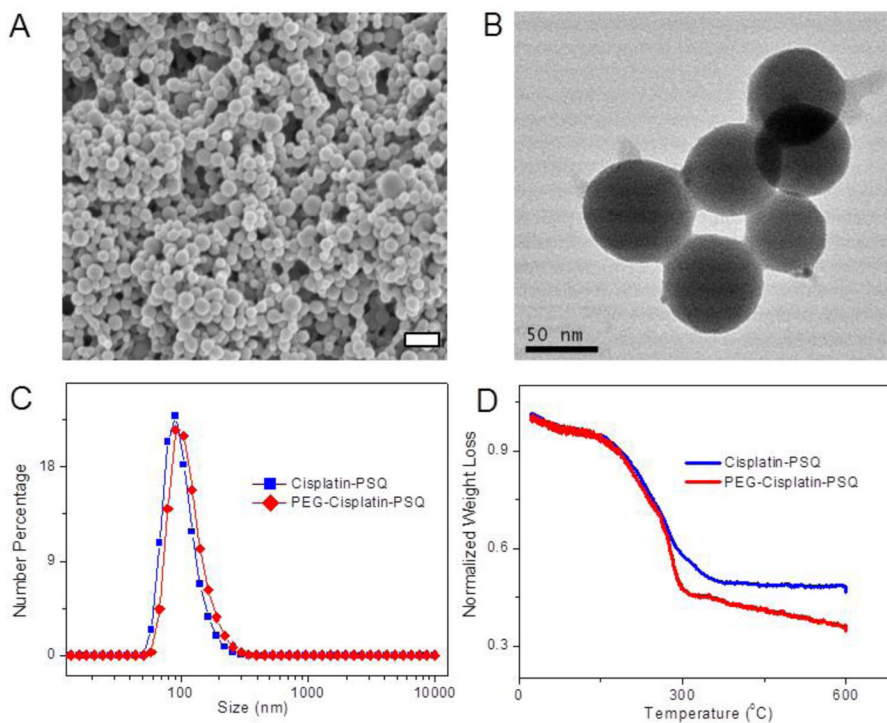


Figure 2.
 a) SEM image of Cisplatin-PSQ NPs (scale bar = 100 nm). b) TEM image of Cisplatin-PSQ NPs (scale bar = 50 nm). c) Number weighted DLS curves for Cisplatin-PSQ (blue) and PEG-Cisplatin-PSQ (red) taken in 5mM PBS (pH=7.4). d) TGA curves of Cisplatin-PSQ (blue) and PEG-Cisplatin-PSQ (red).

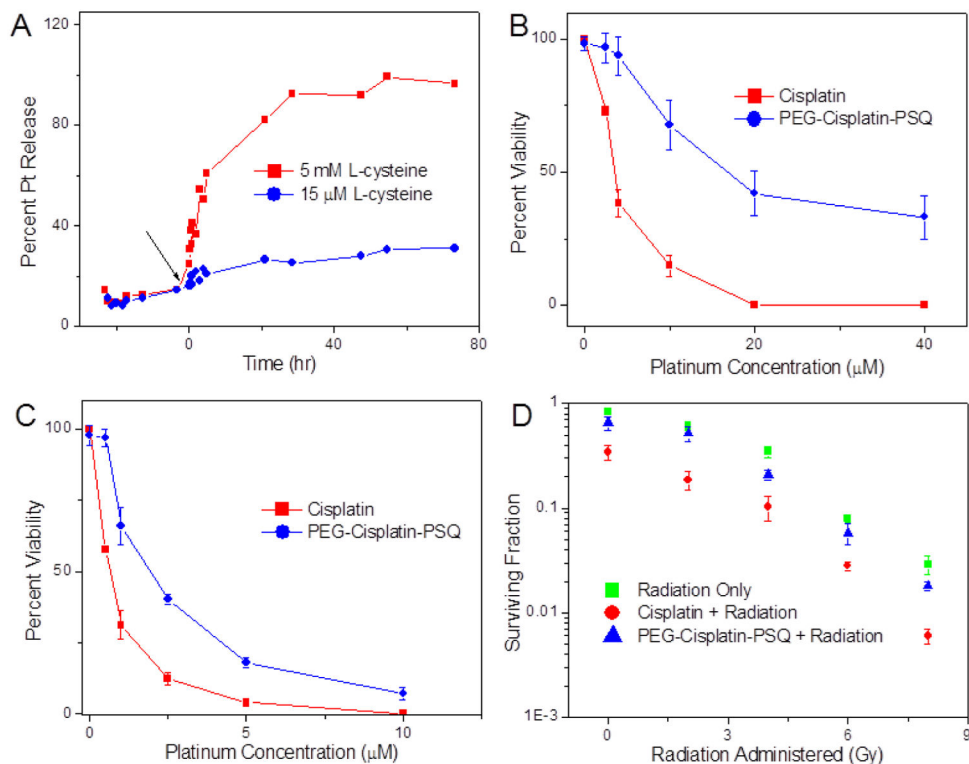


Figure 3.

A) Percentage platinum release from Cisplatin-PSQ in the presence of high (5 mM, red line) or low (15 μM, blue line) concentrations of *L*-cysteine. The reducing agent was added at time 0, indicated by the black arrow. B) Cell viability curves of cisplatin (red, IC_{50} =3.49 μM) and PEG-Cisplatin-PSQ (blue, IC_{50} = 14.91 μM) evaluated in A549 lung cancer cells. C) Cell viability curves of cisplatin (red, IC_{50} =0.65 μM) and PEG-Cisplatin-PSQ (blue, IC_{50} = 2.07 μM) evaluated in H460 lung cancer cells. D) *In vitro* colony forming assay of A549 cells treated with varying doses of radiation only (green), 0.5 μM cisplatin + radiation (red) and 0.5 μM of cisplatin in PEG-Cisplatin-PSQ + radiation (blue).

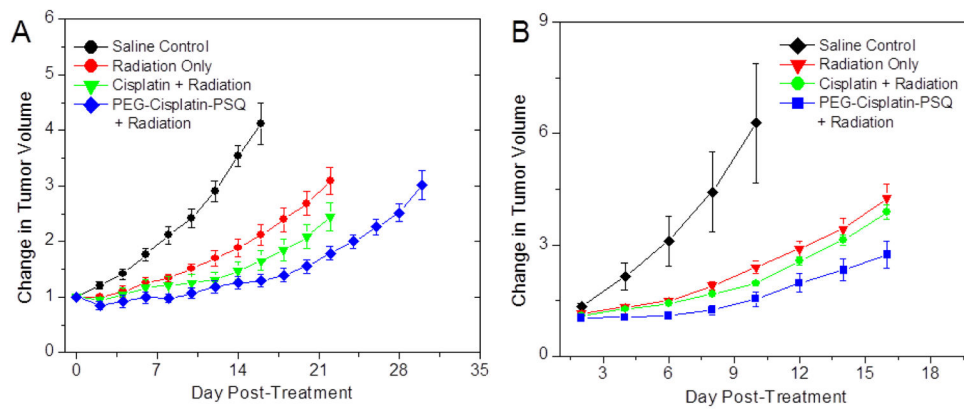


Figure 4. A) *In vivo* chemoradiotherapy efficacy assay against mice bearing A549 xenografts. C) *In vivo* chemoradiotherapy efficacy assay against mice bearing H460 xenografts. Mice received either saline control (black), 10 Gy radiation (red), cisplatin (1 mg/kg) 6 hours prior to 10 Gy radiation (green) or PEG-Cisplatin-PSQ (1 mg cisplatin/kg) 6 hours prior to 10 Gy radiation (blue).

Table 1

Hydrodynamic diameters and zeta potentials of the various Cisplatin-PSQ NPs measured by DLS. All DLS measurements were taken in 5 mM PBS (pH=7.4).

Particle	Z Average (nm)	Polydispersity Index	Intensity Average (nm)	Number Average (nm)	Zeta Potential (mV)
Cisplatin-PSQ	135.2 ± 0.5	0.07 ± .01	147.9 ± 0.8	101.5 ± 0.8	-41.9 ± 2.4
PEG-Cisplatin-PSQ	150.3 ± 5	0.09 ± .01	165.9 ± 5.8	114 ± 5.3	-6.5 ± 0.4